



Experimental Performance Evaluation of a Multi-stream Heat Exchanger for Integration of High-Temperature Steam Electrolysis with Nuclear Reactor Systems

Sin-Yeob Kim¹ · Byung Ha Park¹ · Sung-Deok Hong¹ · Chan Soo Kim¹

Received: 31 March 2024 / Revised: 30 July 2024 / Accepted: 20 August 2024
© The Author(s), under exclusive licence to Korean Institute of Chemical Engineers, Seoul, Korea 2024

Abstract

Printed-circuit type multi-stream heat exchanger was designed and fabricated to produce high-temperature steam and air simultaneously from high-temperature helium heated using the helium loop, which is simulating VHTR (Very-High Temperature gas-cooled Reactor). This study describes the design methodology and the heat transfer performance evaluation results of the multi-stream heat exchanger for stable supply of high temperature steam and air to a 30 kWe SOEC (solid-oxide electrolyzer cell) system to produce hydrogen with high-temperature nuclear reactor systems. In order to control the steam supply above 700 °C, the steam supply control methodology was established with a pressure control valve between the multi-stream heat exchanger and a steam generator. In this study, 20 kg/hr of steam over 800 °C and 110 SLPM of air over 750 °C were supplied stably with the multi-stream heat exchanger using helium loop. The heat transfer performance evaluation for steam is 1.1% below the design condition, which meets the design value within the error range. However, for air, the heat transfer was found to be 50.6% less than the design value due to a decrease in flow rate and reduced heat transfer performance caused by the formation of a deposition layer along the flow path. This high-temperature steam and air supply system will be connected with a high-temperature steam electrolysis system to perform the integral hydrogen production test using helium loop.

Keywords Very-high temperature gas-cooled reactor · Helium loop · High-temperature steam electrolysis · Solid-oxide electrolyzer cell · Printed-circuit type heat exchanger · Hydrogen production · Performance evaluation

List of symbols

A	Area [m ²]
D	Diameter [m]
D_h	Hydraulic diameter (= $4A/P$) [m]
f	Fanning friction factor [-]
h	Heat transfer coefficient [W/(m ² ·K)]
H	Enthalpy [kg·m ² /s ²]
k	Thermal conductivity [W/(m·K)]
L	Flow length [m]
\dot{m}	Mass flow rate [kg/s]
Nu	Nusselt number (= hD_h/k) [-]
p	Pressure [N/m ²]
P	Perimeter of the cross-section [m]
Re	Reynolds number (= $\rho u D_h / \mu$) [-]

T	Temperature [K]
u	Mean velocity [m/s]
x, y	Cartesian coordinates [m]

Greek letters

μ	Dynamic viscosity [kg/(m·s)]
ν	Kinematic viscosity [m ² /s]
ρ	Density [kg/m ³]

Subscripts

c	Cold
f	Fluid
h	Hot
w	Wall

✉ Sin-Yeob Kim
kimsy@kaeri.re.kr

¹ Advanced SMR Technology Development Division, Korea Atomic Energy Research Institute, 111 Daedeok-Daero 989 Beon-Gil, Yuseong-Gu, Daejeon, Korea

Introduction

With recent establishment of carbon reduction goals for carbon neutrality, there is a growing interest in the hydrogen economy [1]. In line with the expansion of the hydrogen

economy, various methods and targets for hydrogen production are being set. At Korea Atomic Energy Research Institute (KAERI), Very High-Temperature Gas-Cooled Reactor (VHTR) has been developed, which is one of the GEN-IV nuclear reactor concepts for large-scale hydrogen production [2]. VHTR can be integrated with various hydrogen production systems requiring high-temperature thermal energy, and High-Temperature Steam Electrolysis (HTSE) is one of the promising hydrogen production technologies, capable of achieving high efficiency under high operating temperature conditions [2].

VHTR can operate at outlet temperatures up to 950 °C by employing helium gas as a coolant, and helium's excellent thermal conductivity makes it suitable for efficiently transferring high-temperature heat. To verify key components of VHTR, KAERI have constructed a helium experimental loop with 600 kW heating power simulating VHTR, and intermediate heat exchanger performance tests were conducted by designing Printed-Circuit type Heat Exchangers (PCHE) [3]. PCHE, made by diffusion bonding materials such as stainless steel, enable highly efficient heat transfer under high-temperature and high-pressure conditions. Compared to shell-and-tube type heat exchangers, they offer a more compact design, providing manufacturing advantages for large-scale heat exchange. Thus, they have been considered as intermediate heat exchangers for high-temperature nuclear reactors [3, 4].

Solid Oxide Electrolysis is anticipated to be one of the most efficient hydrogen production methods within HTSE, using Solid Oxide Electrolyzer Cells (SOECs) under high-temperature operation conditions. This is because the

required electric energy for steam electrolysis decreases as the operation temperature increases [5]. For hydrogen production using SOEC, high-temperature steam and air exceeding 700 °C need to be continuously supplied to the cathode and anode sides of the SOEC stacks, respectively. High-temperature electrolysis under development utilizes electric heating to provide high-temperature steam. However, to make hydrogen cheaper than other fuels, research groups are looking to utilize nuclear thermal energy for hydrogen production [6]. Therefore, it is necessary to demonstrate a high-temperature steam supply system in conjunction with a helium loop for hydrogen production using VHTR, but integrated test study with helium loops and high-temperature electrolysis systems have not yet been conducted.

Based on the accumulated helium loop system technology, KAERI designed a printed-circuit type multi-stream heat exchanger capable of supplying high-temperature steam and air to the HTSE system with SOEC stacks, and aimed to demonstrate hydrogen production by integrating the HTSE with nuclear reactor systems. Figure 1 shows the process flow diagram of the HTSE experiment facility with a helium loop. Helium heated through the helium loop is fed through the printed-circuit type multi-stream heat exchanger and a steam generator to produce high-temperature steam and air, which are supplied to the HTSE system with SOEC stacks to produce hydrogen. This paper describes the design of the multi-stream heat exchanger capable of simultaneously produce high-temperature steam and air from hot helium. In this study, we conducted an experimental performance evaluation of the fabricated multi-stream heat exchanger and confirmed that it can reliably supply high-temperature

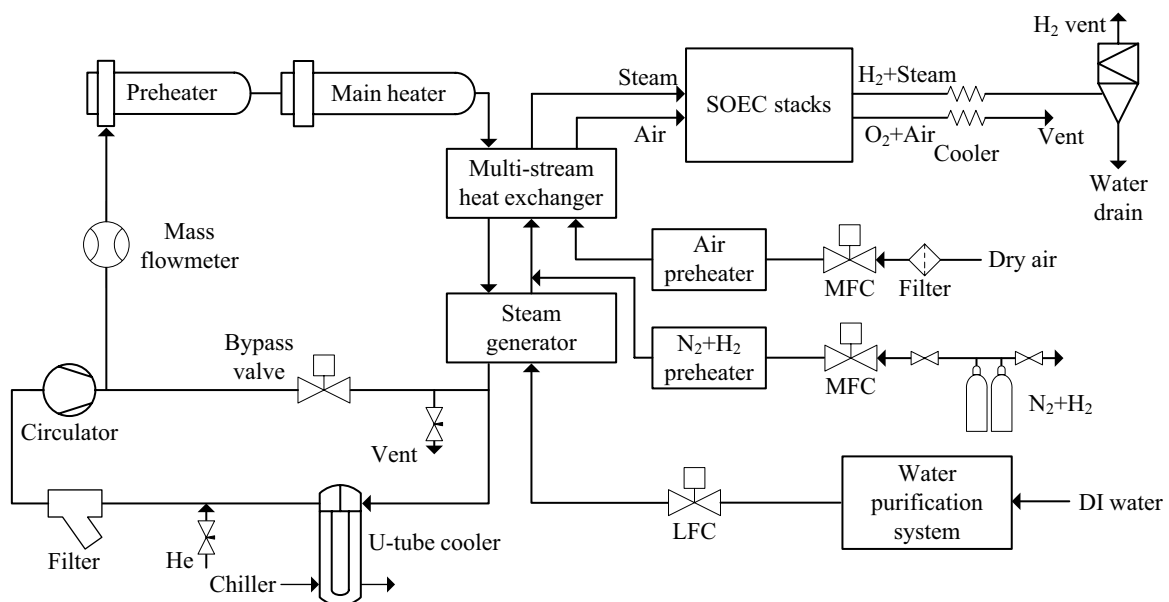


Fig. 1 Process flow diagram of the experiment facility for high-temperature steam electrolysis with helium loop

steam and air. The design condition is to supply steam and air above 700 °C to a 30 kW SOEC system, and the heat transfer performance evaluation results of the multi-stream heat exchanger are reviewed. This high-temperature steam and air supply system would be connected to a SOEC system for a demonstration test of hydrogen production with the helium loop.

Design of the Multi-stream Heat Exchanger

Design Methodology for Printed-Circuit Heat Exchanger

The high-temperature steam production system consists of a steam generator and a superheater. The steam generator is a shell-and-tube type heat exchanger, separated from the superheater to mitigate flow instabilities that can result from the phase change from water to steam. The steam superheater was designed and fabricated as a printed-circuit heat exchanger (PCHE), wherein flow channels are etched onto metallic plates and the plates are diffusion bonded. The steam superheater was designed to transfer heat from helium to steam and air simultaneously, and was called a multi-stream heat exchanger.

Because the VHTRs operate under high-temperature and high-pressure conditions, the PCHEs have been considered as intermediate heat exchangers of the VHTRs to transfer a large amount of heat [3, 4]. PCHEs can be fabricated more compactly compared to shell-and-tube heat exchangers, and as they increase in size to transfer large amounts of heat, PCHEs offer more manufacturing advantages. Its thermal-hydraulic performance and economics are also being studied [7]. Additionally, the diffusion bonding technique used in the fabrication of PCHEs offers better structural integrity and corrosion resistance compared to welding, making it suitable for large-scale high-temperature heat exchange [8]. Furthermore, in this study, to supply high-temperature air and steam simultaneously to the SOEC system, we designed a multi-stream heat exchanger as a PCHE capable of heating both fluids in a single heat transfer component. This study aims to experimentally evaluate the performance

and considerations of this printed-circuit type multi-stream heat exchanger.

The primary considerations in heat exchanger design are the required heat transfer area and pressure drop. The total pressure drop across each fluid system is determined considering the compression ratio of the turbo machinery. The overall pressure drop in the primary system, utilizing helium as the working fluid, cannot exceed 4% of the inlet pressure due to the circulator specification. Considering the system configuration, the pressure drop on the primary side of the heat exchanger was determined to be no more than 2% of the inlet pressure, 40 kPa based on 2 MPa. As the steam and air systems operate at atmospheric pressure in SOEC stacks, the pressure drop for the steam and air were not considered as a major design constraint of the PCHE.

For heat transfer design, an in-house code was developed and utilized. Since significant variations in fluid properties occur within the channels of the heat exchanger, finite difference method was employed for heat transfer analysis [9]. The fluid was modeled in 1D using heat transfer correlations, while the solid was calculated by 2D numerical analysis as described in Fig. 2. The flow boundary condition is adiabatic except where it interfaces with solids. The heat transfer at each node was determined based on changes in enthalpy as follows:

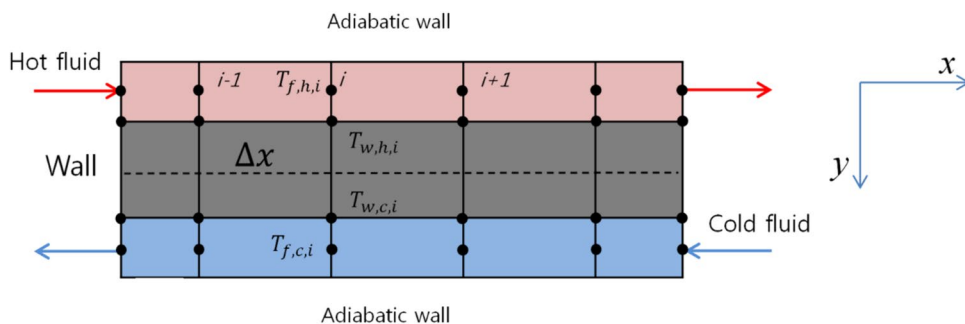
$$\dot{m} \frac{dH}{dx} = hA(T_f - T_w).$$

The equation for the solid part to calculate 2D heat transfer and heat gain or loss to the fluid part is as follows:

$$k_w A_x \frac{\partial^2 T_w}{\partial x^2} dx + k_w A_y \frac{\partial T_w}{\partial y} + hA(T_f - T_w) = 0.$$

In this study, the PCHE flow paths are designed in a semi-circular shape, as shown in Fig. 3. To calculate heat transfer coefficients in the PCHE design program, heat transfer correlations for the Nusselt number based on the flow regime were input for straight and wavy channels angled at 15 degrees in the flow direction with semi-circular cross section [10, 11]. As with the heat transfer correlations, friction

Fig. 2 Finite difference modeling for PCHE design analysis



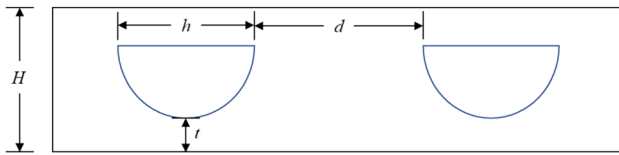


Fig. 3 Design dimensions of PCHE flow paths

factor correlations used for straight and wavy channels with semi-circular cross-sections were also input into the design program [12].

The dimensions considered during the PCHE design process included the thickness of the plates (H), the diameter of the flow paths (h), the spacing between flow paths (d), pressure, and temperature, and so on. For example, optimal design was carried out by examining dimensions where the thickness of the plate was 1 mm or 1.5 mm, and the diameter of the flow paths was 1 mm or 1.5 mm, respectively. The flow paths were designed as wavy channels angled at 15 degrees in the flow direction.

Design of Printed-Circuit Type Multi-stream Heat Exchanger

Design requirements for the multi-stream heat exchanger and the steam generator to produce 820 °C steam and air for a 30 kW SOEC system were derived based on the operational requirements of the helium loop, and they are summarized in Tables 1 and 2. Major design parameters such as the helium outlet temperature of the multi-stream heat exchanger were assumed to be the same as that of the steam generator's helium inlet temperature, and the helium temperature and mass flow rate were obtained using an iterative method.

Considering diffusion bonding characteristics and high-temperature experimental conditions, SS304 material was chosen for the PCHE. SS304 is available for temperatures up to 816 °C according to ASME Sec. VIII [13]. Based on the operational characteristics of the helium loop from fundamental structural dimensions, design conditions of 816°C and 2 MPa were selected, and heat exchanger design was conducted using a diameter of 1.5 mm for the flow channels,

Table 1 Design requirements of the multi-stream heat exchanger

Parameter	Primary side	Secondary side	Third side
Working fluid	Helium	Steam	Air
Inlet pressure [MPa]	2	0.5	0.11
Flow rate [kg/min]	0.42	0.33	0.19
Inlet temperature [°C]	850	155	155
Outlet temperature [°C]	565	820	820
Amount of heat transfer [kW]	- 10.36	+ 8.05	+ 2.31

Table 2 Design requirements of the steam generator

Parameter	Primary side (tube side)	Secondary side (shell side)
Working fluid	Helium	Steam
Inlet pressure [MPa]	2	0.5
Flow rate [kg/min]	0.42	0.33
Inlet temperature [°C]	565	20
Outlet temperature [°C]	163	155
Amount of heat transfer [kW]	- 14.84	+ 14.84

considering pressure drop and flow fouling. Heat exchanger thermal design was carried out using the Logarithmic Mean Temperature Difference (LMTD) method with an empirical margin of 30% considering the configuration of channels and the effect of longitudinal heat conduction. After designing heat exchangers for helium-steam and helium-air systems separately, the final design was determined by adjusting the number of channels per stack to ensure consistency and overall performance. The final size of the heat exchanger core was determined to be $136 \times 52 \times 99 \text{ mm}^3$. To achieve a more uniform temperature distribution, air flow channels were arranged between steam flow channels within the PCHE. At these design conditions, the flow regime for each fluid is laminar, with Reynolds numbers all below 500. In the PCHE design program, the heat transfer coefficient correlation and friction factor used for semi-circular flow paths under laminar flow conditions are $Nu_x = 4.089$ and $f = 16/Re$, respectively [10, 12].

The design configuration and flow patterns of the multi-stream heat exchanger, including headers, are depicted in Fig. 4. Helium flows straight through the paths from the hot end to the cold end to minimize pressure drop in the primary side. Steam and air enter the heat exchanger perpendicularly from the sides and undergo a 90° turn before branching into two streams. To accommodate space constraints, small-sized headers were designed, and flow branching was chosen over straight channels for air and steam. Additionally, to facilitate diffusion bonding at the PCHE core, additional plates within 30 mm of the top and bottom were added, and spaces were provided at the sides for bonding. Figure 5 shows a photograph of the fabricated multi-stream heat exchanger.

High Temperature Steam/Air Supply System

Experiment Facility

Figure 6 illustrates the Process and Instrumentation Diagram (P&ID) of the high-temperature steam/air supply system with helium loop. It is the preliminary experiment

Fig. 4 Design of the printed-circuit type multi-stream heat exchanger and flow paths (A: helium, B: steam, C: air)

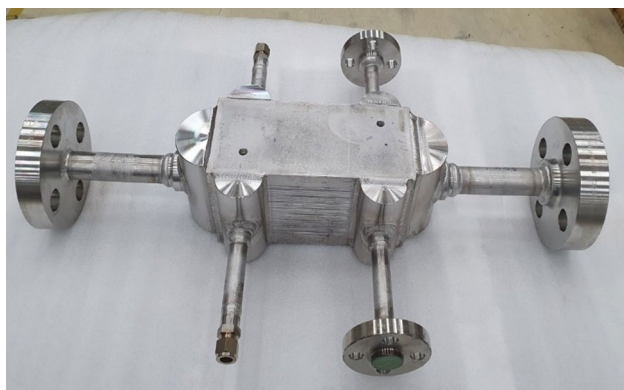
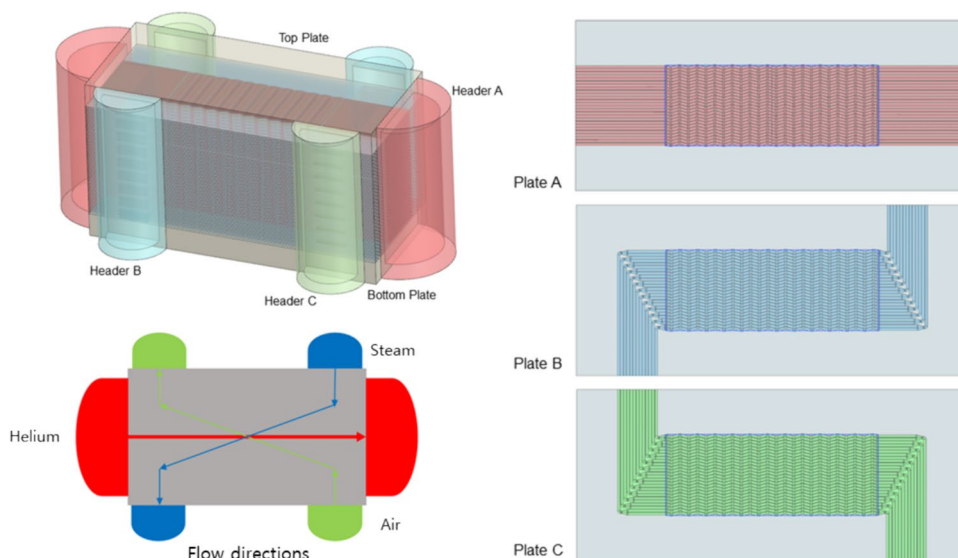


Fig. 5 Fabricated multi-stream heat exchanger

to generate high-temperature steam and air, which will be supplied for the hydrogen production in HTSE system [14]. In this preliminary study without SOEC stacks, the high-temperature steam and air produced through the experiment are exhausted to the outside of the building. This experiment facility is composed of one loop and three lines of different fluids.

- Helium loop (red lines); It circulates high-temperature helium. Via the multi-stream heat exchanger and the steam generator, this loop transfers the heat to generate high-temperature of steam and air for HTSE in SOEC stacks.
- Purified water line (blue lines); It provides purified water to the steam generator with mass flow controller, which controls the water supply and prevents pressure fluctuations due to pump operation.

- Steam line (orange lines); It provides superheated steam from the steam generator to the multi-stream heat exchanger. The steam supply is controlled by a pressure control valve (PCV), which controls the pressure at the top of the steam generator to supply a constant amount of steam to the multi-stream heat exchanger and discharge excess steam to the outside.
- Air line (green lines); It supplies dry air to the HTSE system. Air is heated up through the multi-stream heat exchanger, and it is used as sweep gas of anode side in SOEC stacks. A preheater was used to meet the air inlet temperature condition of the multi-stream heat exchanger.

Figure 7 shows the experiment facility for high-temperature steam and air supply with helium loop constructed with the designed heaters and heat exchangers. It is intended to reduce heat losses through insulation, and a heating jacket was used to compensate for heat losses for the multi-stream heat exchanger, made of ceramic wool and equipped with an embedded heating element, allowing temperature control via PID (Proportional-Integral-Derivative) control.

Instrumentation and Control

The helium flow rate of the helium loop is controlled through the circulator and flow bypass valve, and the flow rate is measured by Coriolis flowmeter. The cooler of the helium loop uses water coolant on the secondary side, which is cooled through the chiller, as described in Fig. 6.

The pressure and differential pressure in the helium loop were measured using Rosemount pressure transmitters with an error of $\pm 0.025\%$. Although not depicted in Fig. 6, the Rosemount differential pressure gauges were

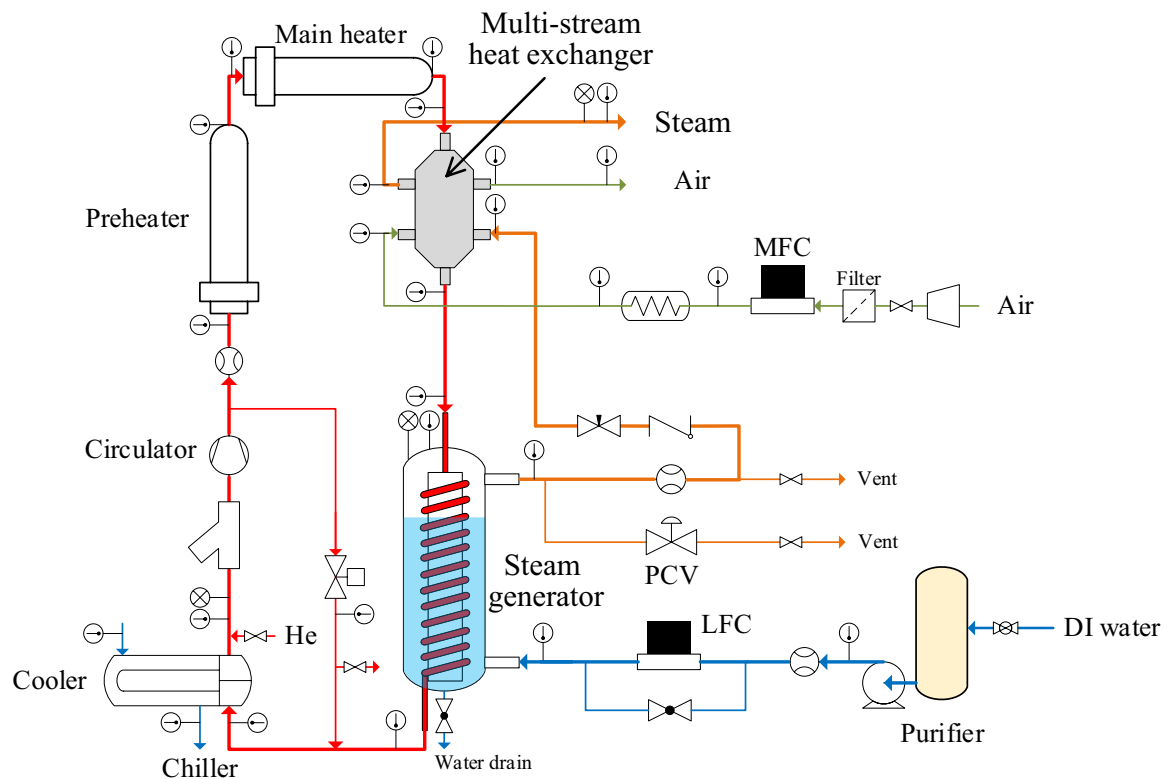
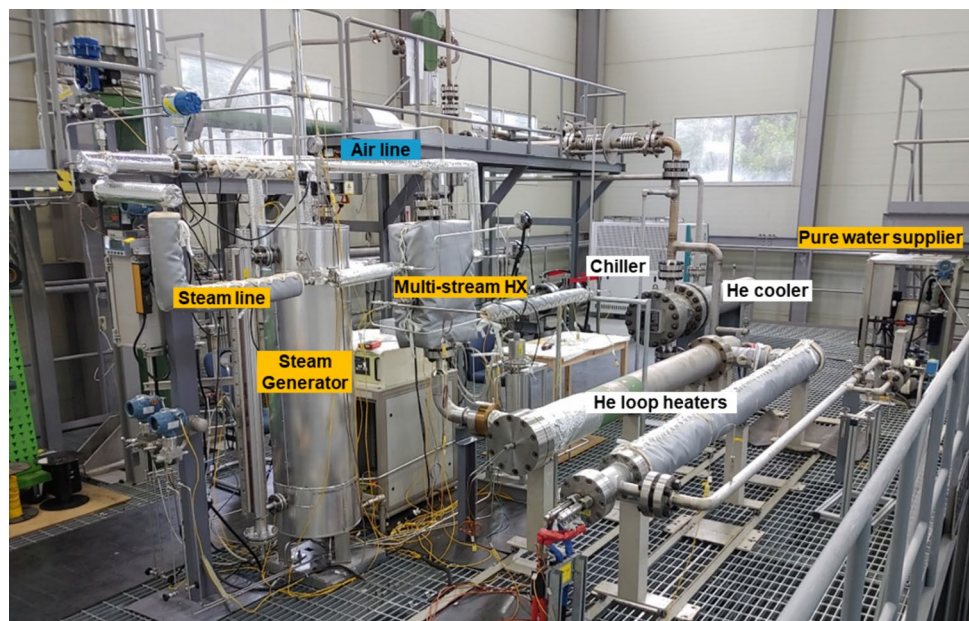


Fig. 6 P&ID of the high temperature steam/air production test facility with helium loop

Fig. 7 Constructed high-temperature steam/air production test facility with helium loop



used to measure the pressure difference of each fluid passing through the steam generator and the multi-stream heat exchanger. The upper plenum pressure of the steam generator was measured using WIKA pressure gauges with an

error of 0.1%, and it is used to control the PCV (PN9000-15 mm, Spirax Sarco) for steam vent.

For stable operation of the steam generator, a Liquid Flow Controller (LFC) (KC-30 K, Alicat CODA) is employed

to maintain a constant flow rate for the target water level inside the steam generator. In the pure water supply system, de-ionized water passes through a water purifier and is pressurized up to 10 bar using a pressure pump. LFC also absorbs pressure fluctuations with a pressure regulator due to intermittent operation of the pressure pump. To measure the flow rate of the vented steam, a vortex flowmeter (KTV-700, KOMETER) was installed along the steam vent line. Linetech's Mass Flow Controller (MFC) was used for air supply. Temperature measurement was conducted using WATLOW's K-type thermocouples.

As illustrated in Fig. 6, the shell and helical tube type steam generator was adopted in this experiment. Heated helium flows inside the tube, while pure water is injected into the shell side. Water partially fills the steam generator, where it is heated and evaporates in submerged area, while steam is superheated in exposed area. Through preliminary experiments, it was confirmed that the water level in the steam generator directly influences both the steam generation rate and the steam superheating. Specifically, lower water levels lead to decreased steam generation and increased superheating, while higher water levels result in increased steam generation and reduced superheating. Therefore, maintaining a consistent water level is crucial for supplying steam at a constant temperature and flow rate. The following outlines the steam supply control methodology established in this study to ensure steady-state conditions with the experiment facility [15].

1. Under ideal steady-state conditions, supplied water and generated steam should be equal. In this state, as the water supply rate decreases, the water level decreases, maintaining a condition where the steam generation rate exceeds the water supply rate and eventually equalizes with it. Likewise, when the water supply rate increases, the water level rises, equalizing with both the water and steam supply rates.
2. After controlling the steam generation rate and steam superheat through water supply, the power of the heaters in the helium loop and the flow rate of helium are controlled based on the temperature of helium and the required heat input.
3. The PCV maintains pressure in the upper plenum of the steam generator, ensuring a stable steam supply to the multi-stream heat exchanger. In this experiment, steam is discharged for two primary reasons. Firstly, to achieve steam outlet temperature over 800 °C for the multi-stream heat exchanger, the inlet temperature of helium should exceed the target temperature and overproduced steam must be vented. Therefore, steam discharge is required for high-temperature steam generation tests over the designed steam flow rate range of the heat exchangers. This allows for a consistent supply of

steam to the multi-stream heat exchanger through PCV, minimizing the influence of changes in steam generator helium inlet temperature due to variations in steam supply. Secondly, to protect the measurement devices, such as the vortex flowmeter and PCV, their operating temperatures must remain below 250 °C. Overproduction of the steam and its discharge serve the purpose of safeguarding the equipment under various flow conditions.

4. Once the flow rates and temperatures of steam and air generated through the multi-stream heat exchanger meet the targets, the helium inlet temperature of the steam generator is determined. This enables the estimation of the heat supply capacity of the steam generator. The supplied heat is mostly utilized for evaporation rather than superheating water or steam. Therefore, supplying the amount of water corresponding to the heat transfer ensures the system operates under steady-state conditions.

The heating jacket temperature of the multi-stream heat exchanger is set to 500 °C to compensate for heat loss (maximum power approximately 2 kW). Air to the superheater is supplied with a target inlet temperature of 200 °C. A 5 kW air heater connected to an AC power supply is used for manual control.

Results

High-Temperature Steam/Air Supply Test

As a preliminary test for the high-temperature steam/air production system integrated with the helium loop for high-temperature electrolysis, the performance of the printed-circuit type multi-stream heat exchanger was evaluated through tests to produce high-temperature steam and air. Figures 8, 9, 10, 11 present the data from the high-temperature steam/air production tests. Stable operational conditions were assumed from 9 h onwards from the data acquisition, and continuous operation for one hour was conducted to verify the stability of the operating conditions.

Figure 8 illustrates the inlet and outlet temperatures of each fluid in the multi-stream heat exchanger, showing that the temperatures of each fluid remain constant after 9 h. It is crucial to maintain stable conditions by producing steam at a constant temperature and flow rate in the steam generator and supplying it to the multi-stream heat exchanger. Figure 9 shows the inlet and outlet temperatures of helium, pure water, and steam in the steam generator, while Fig. 10 displays the mass flow rate of pure water supplied to the steam generator and the amount of steam discharged externally, not supplied to the multi-stream heat exchanger. Figure 11

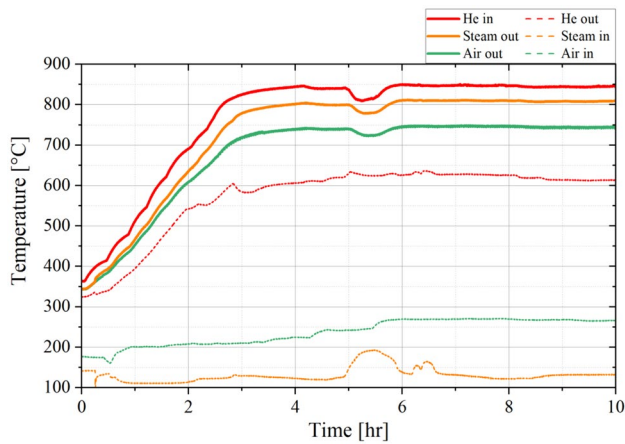


Fig. 8 Temperature results for helium-steam-air multi-stream heat exchanger inlet and outlet by fluid

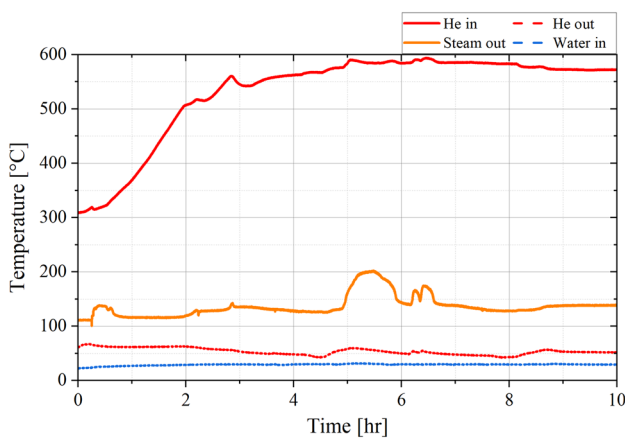


Fig. 9 Temperature results for steam generator inlet and outlet by fluid

illustrates the pressure in the upper plenum of the steam generator.

The stable maintenance of steam outlet temperature, pressure, supply of pure water, and external steam discharge from the steam generator after 9 h confirms that the steam supplied to the multi-stream heat exchanger has reached a steady state condition and was maintained consistently. During the experiment, it was initially considered that steady-state was reached after 7 h. However, it was observed that the water level in the steam generator continued to increase and the steam exit temperature gradually decreased. This indicated that more water was being supplied than the thermal energy helium could transfer. Therefore, we controlled the water supply from 8 to 9 h as shown in Fig. 10, and reviewed the heat transfer amount to ensure all variables reached a steady state. Through these experiments, it was confirmed that the test facility integrated with the helium

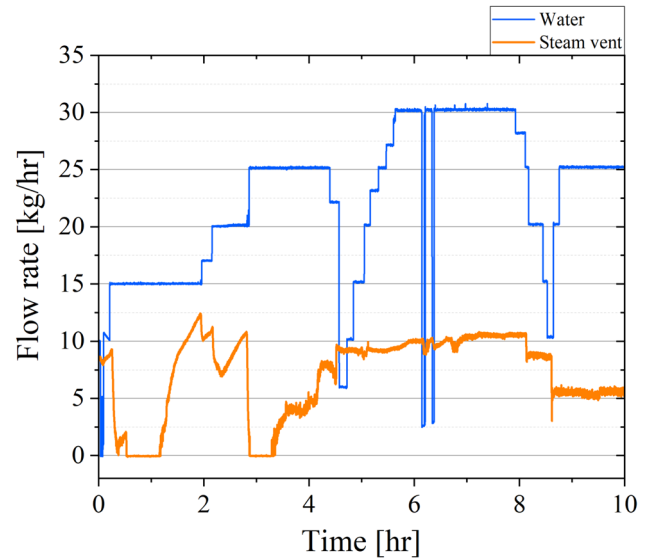


Fig. 10 Mass flow rate of purified water supplied to the steam generator and vented steam

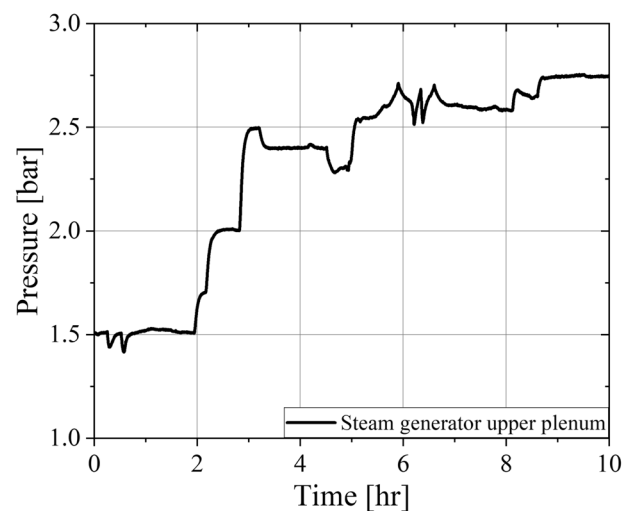


Fig. 11 Pressure results at the upper plenum of the steam generator

loop can reliably generate and supply steam exceeding 800 °C and air at around 750 °C.

Performance Evaluation Results

Table 3 summarizes the test results with the average values and 95% confidence interval of the steady-state conditions for 1 h in the steam generator and the multi-stream heat exchanger compared with the design values. The confidence interval of temperature measurements being within 5 K or less allowed us to confirm that the system was in a steady state during the one-hour period. Table 4 presents the comparison of the heat transfer performance test results obtained

Table 3 Test results compared with the design

Parameter	Design	Test result
Heat transfer device	Multi-stream heat exchanger	
Helium flow rate [kg/min]	0.42	0.418 ± 0.004
Helium pressure [bar]	20	33.83 ± 0.07
Helium inlet temperature [°C]	850	844.4 ± 1.7
Helium outlet temperature [°C]	564.5	613.2 ± 1.0
Steam flow rate [kg/hr]	20	19.7 ± 0.5
Steam inlet temperature [°C]	155	132.0 ± 0.8
Steam outlet temperature [°C]	820	808.2 ± 1.0
Air flow rate [SLPM]	160	109.6 ± 6.3
Air inlet temperature [°C]	155	266.4 ± 2.3
Air outlet temperature [°C]	820	744.3 ± 1.2
Heat transfer device	Steam generator	
Helium inlet temperature [°C]	564.5	572.2 ± 0.8
Helium outlet temperature [°C]	155	52.4 ± 0.9
Water flow rate [kg/hr]	20.16	25.22 ± 0.06
Water inlet temperature [°C]	20	29.7 ± 0.6
Steam pressure [bar]	5	2.75 ± 0.01
Boiling temperature [°C]	151.8	130.6
Steam outlet temperature [°C]	155	138.4 ± 0.8

Table 4 Heat transfer results compared with the design

Parameter	Design	Test result
Heat transfer device	Multi-stream heat exchanger	
Helium heat transfer [kW]	10.36	8.36
Steam heat transfer [kW]	8.05	7.96
Air heat transfer [kW]	2.31	1.14
Heat loss [kW]	–	–0.74
Heat transfer device	Steam generator	
Helium heat transfer [kW]	14.84	18.77
Water/steam heat transfer [kW]	14.84	18.31
Heat loss [kW]	–	0.46

from the experimental results with the design values. The pressure of the helium loop increased from the design pressure of 20 bar to about 34 bar to achieve the target helium flow rate, due to the increased pressure drop from the Coriolis mass flowmeter measuring the helium flow rate. From the experimental results, it was observed that the helium temperature between the outlet of the multi-stream heat exchanger and the inlet of the steam generator, assumed to be the same in the design process, decreased by approximately 40 °C due to heat losses.

From the heat transfer test results in Table 4, it is noted that the steam heat transfer in the multi-stream heat exchanger is 1.1% lower than the design value. However, this discrepancy falls within the measurement error range of the steam flow rate, so it can be considered as meeting the performance target. While passing through the multi-stream heat exchanger from the inlet to the outlet, the steam

temperature increased to 676.2 °C in the experiment, exceeding the design value of 665 °C.

The reason for the negative heat loss in the test result is attributed to the effect of the heating jacket encasing the heat exchanger to compensate for heat losses. The temperature condition of the heating jacket was set to 500 °C to roughly match the helium outlet temperature condition of the multi-stream heat exchanger. However, the high-temperature parts of each fluid are around 800 °C, while the inlet temperatures of steam and air average around 200 °C. Consequently, there is a significant local temperature difference within the multi-stream heat exchanger. Therefore, the experimentally observed negative heat losses are attributed to the influx of thermal energy from the heating jacket specifically into the low-temperature inlet regions of steam and air.

Unlike steam, the air heat transfer performance in the multi-stream heat exchanger was observed to be 50.6% lower

than the design value. This was due to the blockage of the air flow path during repeated high-temperature experiments, likely caused by high-temperature oxidation or carbonization. As the air flow paths narrowed, the pressure difference of the air in the multi-stream heat exchanger continued to increase. Eventually, as the pressure drop in the air flow path began to exceed the supply pressure of the air, the target air supply flow rate could not be met, resulting in a 31.5% decrease in the supplied air flow rate, from 160 SLPM to about 110 SLPM. Despite the decrease in air flow rate, the outlet temperature of the air in the multi-stream heat exchanger did not reach the designed target of 820 °C, even with the air inlet temperature raised to above 260 °C through preheating. This means that heat transfer through the air flow paths is also worsened than designed. Further discussion related to the flow channel pressure drop of the printed-circuit type multi-stream heat exchanger is conducted in Sect. 4.3.

Regarding the steam generator, it was confirmed that the steam production heat transfer performance exceeds the design by 23.4%. The low heat loss of 2.5% in water/steam heat transfer is because the high-temperature helium flows through the helical tube surrounded by water and steam. The excess heat transfer performance of the steam generator is attributed to approximately 25% increased water flow supply, intended to prevent excessive steam superheat at the outlet. The control of the steam generator's upper plenum pressure using the PCV ensures stable supply of the target steam flow rate supplied to the multi-stream heat exchanger.

The difference in steam supply pressure between the design conditions and the test results is attributed to the direct discharge of steam to the building exterior from the rear of the multi-stream heat exchanger, determined by the pressure drops through the flow channels and piping. Computational analysis was conducted using the PCHE design program to confirm the effect of pressure on heat transfer performance of the multi-stream heat exchanger.

If the mass flow rate and temperature conditions remain constant, the product of density and velocity is constant, and the Reynolds number ($Re = \rho u D_h / \mu$) is determined by the dynamic viscosity. However, the dynamic viscosity of steam at 500 °C between the pressures of 2 bar and 5 bar differ by less than 0.1%, about 28.57×10^{-6} kg/(m·s), so the Reynolds number remains constant [16]. In the PCHE design program, the heat transfer coefficient is determined by the Reynolds number, so there is almost no effect on the heat transfer coefficient depending on the pressure of the steam. Furthermore, because the flow paths of the multi-stream heat exchanger were designed under laminar flow conditions, $Nu = 4.089$ for the steam flow [10]. Therefore, the PCHE design program showed a difference of less than 1 °C in the steam outlet temperature of the multi-stream heat exchanger, even with varying steam pressure conditions. This indicates that

even in conditions of low pressure for high-temperature electrolysis testing, where relatively small amounts of steam are supplied, the heat transfer performance of the multi-stream heat exchanger would not be reduced.

Pressure Drop Across the Multi-stream Heat Exchanger

Using the PCHE design program, the pressure drop for each fluid under the design conditions of the multi-stream heat exchanger is as follows: 2.7 kPa for helium, 1.3 kPa for steam, and 2.1 kPa for air. Through repeated experiments, it was observed that the pressure drop in both the steam and air flow paths tended to increase with each high-temperature test. The pressure drop in laminar flow conditions is as follows [12]:

$$\Delta p = \frac{1}{2} \rho u^2 \frac{4L}{D_h} f = \frac{32\nu L \rho u}{D_h^2}$$

In the PCHE, the flow length (L) remains constant, and when the mass flow rate is constant, the ρu varies inversely with the flow cross-sectional area (A) according to the following equation:

$$\rho u = \dot{m}/A$$

Therefore, when the mass flow rate and temperature are the same, the pressure drop in the PCHE's flow paths under laminar flow conditions is inversely proportional to the square of the cross-sectional area of the flow paths. The measured pressure drops for each fluid in the tests presented in this paper are as follows: 2.5 kPa for helium, 52.7 kPa for steam, and 225.3 kPa for air. The differential pressure of helium was found to be lower than the design value, while that of the steam deviated from the design value by about 40 times and that of the air by more than 100 times, even though the experimental and design conditions such as flow rate are different to fulfill other operating conditions in the experiment. Therefore, it is inferred that the flow paths of the PCHE may have narrowed due to high-temperature oxidation or carburization in repeated high-temperature experiments.

To verify this, the flow paths at the inlet and outlet of the multi-stream heat exchanger were observed using a bore-scope camera. Through this, it was confirmed that part of the steam and air flow channel outlets of the multi-stream heat exchanger were blocked by oxides, which would contribute to the increase in pressure drop along the steam and air flow paths.

These deposits can also accumulate on the flow channel walls and affect the heat transfer rate between fluids. As discussed in Sect. 4.2, the mass flow rate of the air supplied to the multi-stream heat exchanger decreased by only 31.5%, but the heat transfer to the air decreased by 50.6%. It

Table 5 Thermal conductivity of the steam and air at 1 bar for various temperatures [16]

Temperature [°C]	Thermal conductivity of steam [mW/(m·K)]	Thermal conductivity of air [mW/(m·K)]
200	33.43	38.25
300	43.53	44.42
400	54.65	50.24
500	66.59	55.80
600	79.17	61.14
700	92.28	66.31
800	105.81	71.35

is estimated that the deposits are the reason for a significant reduction in the heat transfer rate in the air flow channel. However, simply identifying the deposits at the inlet and outlet of the flow paths is not sufficient to determine the extent of the deposits along the flow path and to quantify their influence on the heat transfer rate. Therefore, further research is needed to understand the causes of these deposits and to implement design improvements that take them into account.

Additionally, despite a significant increase in the pressure drop in the steam flow path, as in the air flow path, the heat transfer to the steam did not decrease significantly in Table 4. This is likely because the deposition layer in the steam flow path is thinner than that in the air flow path, and as shown in Table 5, the thermal conductivity of steam is significantly higher than that of air at high temperature condition. Therefore, it is estimated that the effective overall heat transfer coefficient between the helium and steam, including the deposition layer, remains higher than the convective heat transfer coefficient of steam. In the future, the heat exchanger will be disassembled and the composition of the deposition will be analyzed to confirm the material and the cause of their formation.

In this study, the experimental performance evaluation of the PCHE designed to supply high-temperature steam and air to a 30 kW SOEC was conducted. We confirmed the heat exchange performance of the PCHE and its ability to control and supply flow rates stably. Additionally, based on the established methodology and the discussion, an additional test for supplying high-temperature steam and air to a 6 kW SOEC was carried out, although it is not covered in this paper. It was confirmed that the experiment facility could heat the steam and air up to 700 °C under lower flow rate conditions, even if deposits accumulated inside of the flow paths of the multi-stream heat exchanger. In the future, this high-temperature steam/air supply system will be connected to a 6 kW SOEC system to conduct hydrogen production demonstration tests.

Conclusions

In this study, a printed-circuit type multi-stream heat exchanger, capable of producing high-temperature steam and air using a helium loop, was designed and the performance evaluation of the heat exchanger was conducted. The multi-stream heat exchanger was designed to perform 30 kW high-temperature electrolysis, with steam mass flow rate of 20 kg/hr and air mass flow rate of 11.52 kg/hr (160 SLPM). The design temperatures for the inlet and outlet of steam and air are 155 and 820 °C, respectively. Accordingly, the heat transfer rates for steam and air are 8.05 kW and 2.31 kW, respectively, totaling 10.36 kW. As a preliminary test for the high-temperature electrolysis test integrated with the helium loop, the high-temperature steam and air supply system with the multi-stream heat exchanger was constructed and tested. To stably control the steam flow rate before the multi-stream heat exchanger, a pressure control valve was installed and the steam supply control methodology was established. Through performance evaluation tests, it was confirmed that the test facility could stably supply over 800 °C steam at a rate of 20 kg/hr and about 750 °C air at a rate of 110 SLPM. The heat transfer rates of steam and air were determined to be 7.96 kW and 1.14 kW, respectively. While the steam heat transfer rate meets the design conditions within the measurement error range, the air heat transfer rate is approximately 51% lower than the design due to blockage of the air flow channels in the multi-stream heat exchanger, resulting in a decrease in the mass flow rate supplied by approximately 32% due to increased pressure drop in the flow channels. In the future, this high-temperature steam and air supply facility would be connected to a 6 kW high-temperature electrolysis system to perform an integral test of hydrogen production, and the operating conditions of the integral test facility with solid-oxide electrolyte cell stacks would be reviewed.

Acknowledgements This work was supported by the National Research Foundation of Korea (NRF) grant funded by the Korea government (MSIT) (Grant Code: 2021M2D4A2046777).

Data availability The data for this study is available upon request from the authors.

References

1. A. Kim, H. Lim, Economics and sustainability of introducing clean hydrogen from Australia in the Republic of Korea. *Korean J. Chem. Eng. Chem Eng.* **41**(9), 2525–2539 (2024)
2. J.H. Chang, Y.W. Kim, K.Y. Lee et al., A study of a nuclear hydrogen production demonstration plant. *Nucl. Eng. Tech.* **39**, 111 (2007)

3. C.S. Kim, J.S. Chae, S.D. Hong, *Performance test of very high temperature helium experimental loop* (Proc. of the International Congress on Advances in Nuclear Power Plants, Jeju Island, 2013), pp.14–18
4. Peterson PF, Zhao H, Fukuda G, “Functional Requirements Overview For a 50-MW(t) Liquid-Salt Intermediate Loop for NGNP, Report UCBTH-05–007, U. C. Berkeley, pp. 1–12, (2005).
5. M.A. Laguna-Bercero, Recent advances in high temperature electrolysis using solid oxide fuel cells: a review. *J. Power. Sources* **203**, 4–16 (2012)
6. Boardman RD, Westover TL, Remer SJ, “Plan for Scaling Up Hydrogen Production with Nuclear Power Plants,” INL/RPT-22–68155, Revision 0, (2022).
7. S.W. Lee, S.M. Shin, S. Chung, H. Jo, Evaluation of thermal-hydraulic performance and economics of Printed Circuit Heat Exchanger (PCHE) for recuperators of Sodium-cooled Fast Reactors (SFRs) using CO₂ and N₂ as working fluids. *Nucl. Eng. Technol. Eng. Technol.* **54**, 1874–1889 (2022)
8. I.H. Kim, X. Zhang, R. Christensen, X. Sun, Design study and cost assessment of straight, zigzag, S-shape, and OSF PCHEs for a FLiNaK-SCO₂ secondary heat exchangers in FHRs. *Ann. Nucl. EnergyNucl. Energy* **94**, 129–137 (2016)
9. Versteeg HK, Malalasekera W, *An Introduction to Computational Fluid Dynamics: The Finite Volume Method 2nd Edition*, PEARSON Education, England, (2007).
10. N.R. Rosaguti, D.F. Fletcher, B.S. Haynes, Laminar flow and heat transfer in a periodic serpentine channel with semi-circular cross-section. *Int. J. Heat and Mass Transfer* **49**, 2912–2923 (2006)
11. I.H. Kim, N.O. HeeCheon, Thermal-hydraulic physical models for a printed circuit heat exchanger covering He, He-CO₂ mixture, and water fluids using experimental data and CFD. *Exper Thermal Fluid Sci.* **48**, 213–221 (2013)
12. S.W. Churchill, Friction factor equations spans all fluid-flow regimes. *Chem. Eng. J.* **84**, 91–92 (1977)
13. ASME, ASME Boiler and Pressure Vessel Code Section VIII, Mandatory Appendix, (2015).
14. Kim SY, Hong SD, Park BH, Kang KJ, Kim HS, Kim CS, “Design and Construction of the Experiment Facility for the High-Temperature Steam Generation with Helium for 30kW High-Temperature Steam Electrolysis,” Proc. of 20th International Topical Meeting on Nuclear Reactor Thermal Hydraulics, Washington, D.C., USA. pp. 1476–1487 August 20–25, (2023).
15. S.Y. Kim, S.D. Hong, K.J. Kang, C.S. Kim, *Experimental study on the high-temperature steam supply system using helium loop for reliable steam generation control* (Trans. of the Korean Society Spring Meeting, Jeju, 2023), pp.18–19
16. Lemmon Eric W., et al. “NIST standard reference database 23: reference fluid thermodynamic and transport properties-REFPROP, Version 10.0, National Institute of Standards and Technology.” Standard Reference Data Program, Gaithersburg (2018).

Publisher's Note Springer Nature remains neutral with regard to jurisdictional claims in published maps and institutional affiliations.

Springer Nature or its licensor (e.g. a society or other partner) holds exclusive rights to this article under a publishing agreement with the author(s) or other rightsholder(s); author self-archiving of the accepted manuscript version of this article is solely governed by the terms of such publishing agreement and applicable law.